Optomechanical measurement of the role of Lamins in whole cell deformability

Optomechanical measurement of the role of lamins in whole cell deformability

Thorsten Kolb[1,2], Julia Kraxner[1], Kai Skodzek[3], Michael Haug[1], Dean Crawford[3], Kendra K. Maaß[2], Katerina E. Aifantis[4,5], and Graeme Whyte[1,3]*

[1]Department of Physics, Friedrich-Alexander-Universität Erlangen-Nürnberg, Henkestrasse 91, 91052 Erlangen, Germany

[2]Division of Molecular Genetics, Deutsches Krebsforschungszentrum, Im Neuenheimer Feld 580, 69120, Heidelberg, Germany

[3]Institute of Biological Chemistry, Biophysics and Bioengineering, Heriot-Watt University, Edinburgh, EH14 4AS, UK

[4]Lab of Mechanics and Materials, Aristotle University of Thessaloniki, 54124 Thessaloniki, Greece

[5]Department of Civil Engineering-Engineering Mechanics, University of Arizona, Tuscon, Arizona 85721

Receivedzzz, revisedzzz, acceptedzzz
Published online zzz

Key words: Optical Stretcher, Single-Cell Analysis, Cell Mechanics, Nuclear Envelope, Lamin A

There is mounting evidence that the nuclear envelope, and particularly the lamina, plays a critical role in the mechanical and regulation properties of the cell and changes to the lamina can have implications for the physical properties of the whole cell. In this study we demonstrate that the optical stretcher can measure changes in the time-dependent mechanical properties of living cells with different levels of A-type lamin expression. Results from the optical stretcher shows a decrease in the deformability of cells as the levels of lamin A increases, for cells which grow both adherently and in suspension. Further detail can be probed by combining the optical stretcher with fluorescence microscopy to investigate the nuclear mechanical properties which show a larger decrease in deformability than for the whole cell.

1. Introduction

The nuclear envelope builds the outermost layer of the nucleus and harbours the nuclear pore complexes, a plethora of membrane spanning proteins and the nuclear lamina, a fibrous meshwork of type V intermediate filaments termed the nuclear lamins (for review see [1]). Many of the interactions between the extra-cellular world, the cytoskeleton, and the DNA occur via trans-membrane proteins that link the lamina to the cytoskeleton [2] and it is fundamental in a series of basic cellular processes[3–7]. In human somatic cells four main lamin molecules, lamin A, B1, B2 and C, can be found, and especially lamin A was shown to be important for nuclear integrity [8], organisation of the nuclear pore complexes, gene expression and chromatin localisation [9–11].

Several very sensitive techniques are available to measure cell mechanics – atomic force microscopy[12,13], micropipette aspiration [14] and bead-based measurement using optical[15] or magnetic[16] forces. However, most of these techniques deliver very low throughputs in the order of a few cells per hour. At the other end of the spectrum, there have been a number of recent developments using the fast flowing nature of microfluidics to measure the mechanical properties of cells including real-time deformability cytometry[17] and hydrodynamic stretching[18,19], which are capable of measuring up to 100 and 2,000 cells/s respectively, however their ability to detect time-dependant changes in the stiffness is limited.

The optical stretcher[20] sits between these two extremes, providing detailed time dependent measurements of the mechanical response of cells at a throughput of around 100 cells per hour. It has been shown to be sensitive to measure changes in stiffness due to cell differentiation[21], activation and stem cell pluripotency[22], and used to investigate the effects of actin, microtubules[23], myosin[24] and keratins[25], however to-date it has not been used to investigate the changes in mechanical properties due to the nuclear lamina.

* Corresponding author: e-mail g.whyte@hw.ac.uk, Phone: +00999999999, Fax: +00999 999999

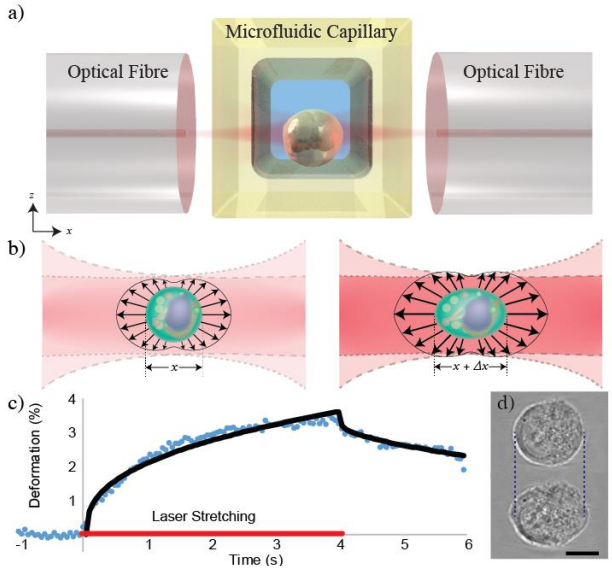

Figure 1 a) Schematic of the optical stretcher comprising two optical fibres perpendicular to a square capillary. b) Schematic of the forces acting upon a cell within the optical stretcher during trapping (left) and stretching (right). The laser axis is parallel to the indicated x axis. c) Example of the deformation response of a single MAF cell during stretching (blue dots) with the corresponding power-law model fit (solid black line) overlaid. d) Images of the cell obtained during stretching showing the deformation along the stretch axis. Scale bar: 10 µm.

2. Experimental

The optical stretcher (OS) is a form of dual-beam optical trap [26,27] arranged such that the trap is positioned across a microfluidic flow channel. With a low optical power, living cells can be held stationary in the trap. By increasing the optical power of the laser, a trapped living cell is subjected to anisotropic stresses on its surface causing it to deform. Monitoring the edge of the cell makes it possible to measure the deformation during the stretching process. The OS has been used to measure mechanical differences between various cell types and disease states. It is sensitive to both, the cytoskeletal and nuclear properties of the cell [21,22,25].

The experimental system is similar to that described elsewhere [28,29]; briefly it consists of two single-mode optical fibres which are arranged on a guide to be co-linear and perpendicular to a square cross-section glass capillary flow cell, as shown in Figure 1. This capillary is connected via microfluidic tubing to fluidic reservoirs, which use either hydrostatic pressure or regulated compressed air to control the flow through the glass capillary.

If a sample containing cells is flowed through the system, it is possible to easily capture individual cells in the optical trap. Once a cell is trapped it can be held in the optical trap with little damage [30–32] and imaged without any artefacts from surface contact.

To investigate if the system was capable of measuring changes in mechanical properties due to different expression levels of A-type lamins, stable cell-lines expressing different levels of the nuclear protein lamin A were measured in the optical stretcher. Adult mouse fibroblast (MAF) cells lacking a functional lamin A gene (*Lmna)*[33] were compared to control cells expressing the fully functional *Lmna* gene and cells which lack the functional *Lmna* gene but were transfected to express polyhistidine-tagged lamin A. To verify the effect was not limited to these cells, or only to adherent cells, the suspension cell line K562 was also modified to express eGFP-coupled lamin A and stable cell lines expressing different levels were established.

3. Results

3.1 Presence of lamins affects cell stiffness

As has been shown [34,35], increased expression of lamins results in increased cellular stiffness. To investigate the capability of the optical stretcher to detect such changes, knock out cells which lack a functional *Lmna* gene were compared to the corresponding wild-type cells. As can be seen in Figure 2, the optical stretcher can clearly differentiate between cells lacking the functional lamin A gene (labelled -/-) and the significantly stiffer corresponding wild type cells (labelled WT). To show that the partial re-expression of A-type lamins can rescue this softening phenotype, stable *Lmna*$^{-/-}$ cells expressing human lamin A, N-terminally fused to a polyhistidine-tag were developed. The deformation profiles of these rescue cells showed deformations in the range between the wild type controls and the knockout cell line, the expression levels of lamin A in both cells are similar, however the total A-type lamin expression level of the rescue cell line was measured to be 63 % ± 7 % (N=3) of the expression level of the control cells when both lamin A and C are taken into account (Figure 2c). By fitting the time dependent deformation with a power law, the initial deformability of the cells with increased lamin A levels decreases, while their viscoelasticity does not change significantly, as shown in Figure 2d.

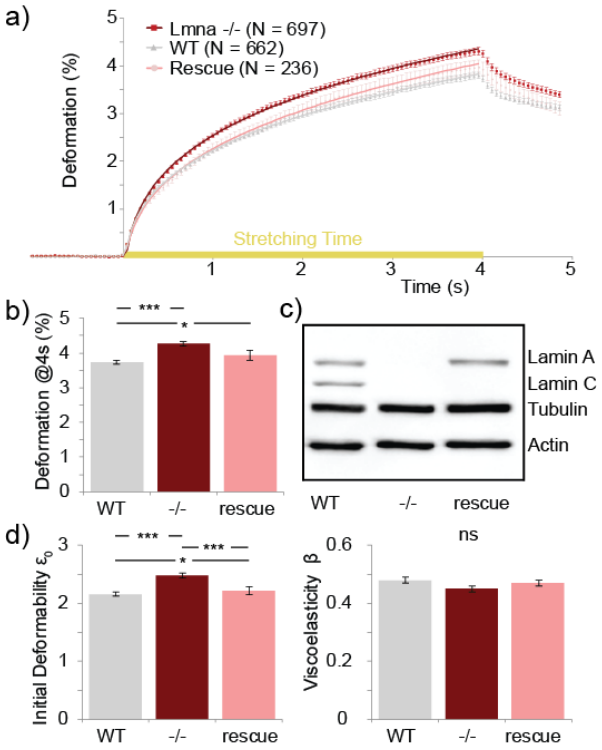

Figure 2 a) Deformation of MAF cells measured in the optical stretcher for the wild-type (WT, grey, N=623 from 7 experiments), cells lacking a functional *Lmna* gene (-/- dark red, N=697 from 9 experiments) and cells lacking a functional *Lmna* gene transfected with polyhistidine-tagged lamin A (rescue, light red, N=236 from 9 experiments). Solid lines represent power-law model fits to the average deformation for each population. b) Deformation at the end of stretching (4s) for each cell type. c) Representative western blot of the proteins encoded by the *Lmna* gene showing the lack of lamin A and C in the knock out, and the reintroduction of lamin A in the rescue cell line. d) Power law fit parameters for each cell type showing the deformability of the cells changes with the presence of lamin A, while the viscoelasticity remains unchanged. Error bars are standard error, * denotes $p<0.05$ while *** denotes $p<0.001$.

3.2 Lmna expression affects nuclear deformation

In order to measure the effect of *Lmna* expression on the nuclear meachanics, the nuclear deformation of wild type and knock-out MAF cells was measured by staining the DNA with Hoechst 33342 dye. This cell permeable dye binds to the nuclear DNA and fluoresces blue when excited with UV light, allowing visualisation of the nucleus during optical stretching.

As shown in Figure 3, the absence of A-type lamins results in increased deformations of the nucleus as is the

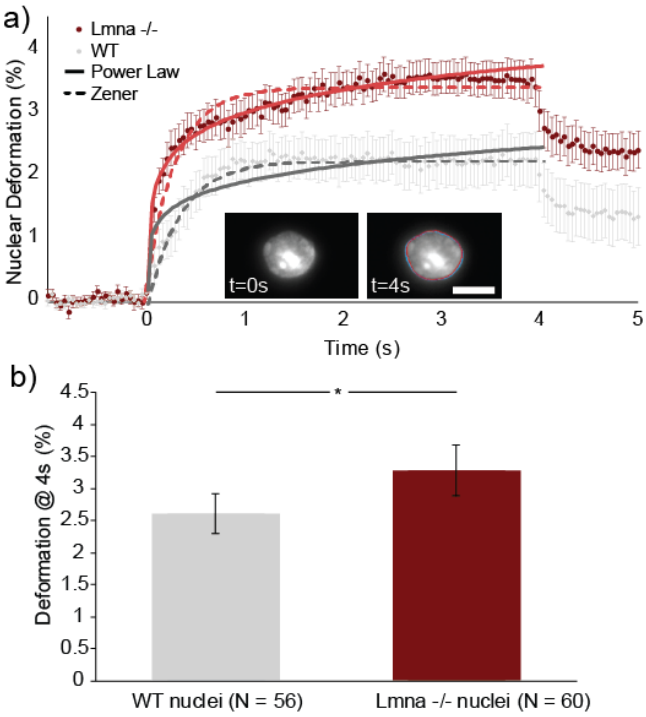

Figure 3 Measurement of the nuclear deformation during optical stretching. a) Deformation curves for the nuclei of MAF cells with the functional *Lmna* gene (grey, WT N=56 from 3 experiements) and MAF cells lacking the functional *Lmna* gene (red, *Lmna* -/- N=60 from 3 experiments). Lines represent model fits: solid line is power law fit similar to whole cell behaviour, while dashed lines represent a Zener Maxwell model. Inset shows fluorescent images of the nucleus during stretching. Red and blue lines denote the edge of the nucleus before and at the end of stretching. b) Deformation at the end of stretching (4 s) showing a significant increase in nuclear deformation in the absence of the functional *Lmna* gene. Error bars are standard error, * denotes $p<0.05$ and the scale bar is 10 μm.

case with the whole cell. Our findings agree qualitatively with studies carried out on Embryonic Mouse Fibroblast cell nuclei with *Lmna* deficiency under uniform biaxial strain[36] and micropipette aspiration measurements on isolated nuclei from HSC/A549 cells [37]. The shape of the deformation curve for the nuclei are different in character to the whole cell curves, with the nuclei deformation reaching a plateau within the 4 s of stretching, thus not following the power-law behaviour of the whole cell and consistent with previous measurements on isolated nuclei[38,39]. In order to compare the properties of the nuclei deformation, a modified Maxwell model, known as Zener model was fitted to the mean deformation[40]. The Lmna -/- nuclei display a large reduction in both the viscous and elastic components, consistent with the increased deformability of the nuclei. While the nuclei display a reduced deformability compared to the whole cell, the change in deformability by removing A-type lamins is more dramatic for nuclear deformation, showing the effect is more significant on the nucleus.

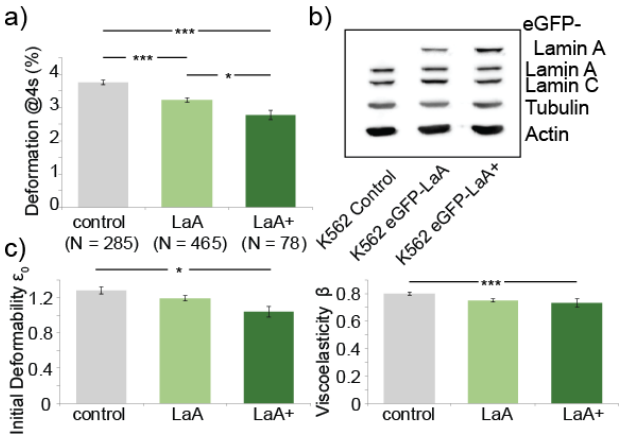

Figure 4 a) Deformation of suspension cell line K562 transfected with different levels of lamin A, wild-type cells (control, grey, N=285 cells from 4 experiments), low levels of eGFP-lamin A expression (LaA, light green, N=465 from 5 experiments) and strong expression (LaA+, dark green, N=78 from 3 experiments). b) Representative western blot analysis of the expression levels of lamin A/C within the different cell lines show constant levels of lamin A and C while levels of eGFP-lamin A are increased in the transfected cell lines. c) Power law fit parameters of the deformation curves showing the decreased initial deformability and similar viscoelasticity for increasing levels of lamin A. * denotes $p<0.05$ and *** denotes $p<0.001$.

3.3 Overexpression of lamin A increases the stiffness of suspension cells

To rule out the measured changes in mechanical properties as an isolated effect from using the MAF cells, a second series of cell lines was established. To investigate the effects of an increased lamin A expression on suspended cells, a stable K562 suspension cell line expressing eGFP-lamin A was generated. Positive cells were FACS sorted to yield two sublines, one with a strong expression level and one with a lower expression of eGFP-Lamin A which could be compared to the control cells.

The deformation profiles, shown in Figure 4, display similar trends as for the adherent MAF lines, showing the deformability decreases with increasing levels of lamin A, suggesting the presence of lamin A increases the stiffness.

4. Discussion

Measurements of the mechanical properties of living cells are becoming an ever more important technique for the marker-free characterisation of cell type and condition. The wide array of cell states and diseases, which can lead to altered mechanical properties, means that the investigative and diagnostic potential of cell mechanics is very large but to enable its full potential, accurate and sensitive techniques are needed.

Therefore, the optical cell stretcher allows for detailed measurement of mechanical properties of cells and can be combined with standard fluorescent techniques to enable a high-content screening of cell populations. The laser based, non-contact method of measurement allows the whole-cell mechanics to be investigated without any contact artefacts, moreover the integration of microfluidics gives a throughput in the range of a 100 cells per hour. While higher-throughput techniques have been developed [17,18,41], their ability to measure the time-dependent mechanical properties are inherently limited by the short measurement time, often only a single time point which may lead to subtle effects being missed.

Lamin A is a major protein of the nuclear envelope, which has roles in stabilising the nucleus against mechanical stresses, nuclear mechanics and gene regulation. It has been linked to a plethora of diseases (for review see [42,43]) and plays a role in the differentiation of cells [14,44] and so being able to measure the changes in a non-destructive way within living cells is an important step forward to a better understanding of the mechanical role of the nuclear lamina.

The results demonstrate that the optical stretcher is a useful tool for investigating changes in mechanical properties of living cells and is sensitive enough to measure changes in whole-cell and nuclear deformability due to differing expression levels of A-type lamins. The observation of decreased deformability with increasing lamin A levels supports previous studies performed with a variety of mechanical measurement techniques[35,36,45–47] and gives researchers another method to rapidly measure alterations in the viscoelastic properties of cells.

Following on from this study, by developing cell systems with altered expression levels of the four main lamin proteins (lamin A, B1, B2 and C), the optical cell stretcher will allow us to perform a fine mapping of the contribution the four main lamin proteins have in whole cell and nuclear mechanics.

In addition, the microfluidic nature of the system can be modified to collect individual cells after being analysed to correlate their mechanical phenotype to the individual gene expression pattern on a single-cell level.

5. Conclusion

We have shown that the optical stretcher can be used to detect changes in the mechanical properties of cells and nuclei in a non-contact manner. The measured changes in

whole cell stiffness correlated with the levels of lamin A/C in both adherent and suspension cell lines, which was successfully shown for both raised and reduced expression of the protein. This capability to detect subtle changes in the internal structure of the nucleus of the cell adds to the potential applications of the optical stretcher as a sensitive probe for detecting the physical properties of living cells.

Acknowledgments

This work was supported through the EAM Rising Star program, the European Research Council Starting Grant (MINATRAN 211166) and the MRC funded ESRIC programme (MRC_MR/K01563X/1). The authors would like to acknowledge Harald Herrmann and Colin Stewart for providing cell lines.

6. Materials and Methods

6.1 Device Fabrication

A dual-beam fibre trap was built as described by Lincoln[28], briefly, a 80 μm ID, 160 μm OD square cross-section capillary (CM Scientific) was aligned perpendicularly to two single mode optical fibres (HI-1060, Thorlabs) using photolithographically defined SU8 (SU8-2025, MicroChem Inc.) guides. The ends of the capillary were connected to PEEK (Upchurch Scientific) tubing using high-pressure microfluidic unions (Upchurch scientific) to allow liquids to be flowed through the system. The single mode fibres were connected to a 1070 nm laser (YLM-1070-5LP, IPG Photonics) via a 50:50 single-mode fibre splitter (Gould Photonics) to provide both sides of the trap from a single laser source. Fluid was driven through the system using a bespoke air-over-liquid pump system connected to the PEEK tubing. The pressure applied to the liquid was regulated using a high-accuracy electronic pressure regulator (Marsh Bellofram) controlled by a DAQ card (National Instruments). The balancing pressure on the other vial was controlled by a manual pressure regulator (Marsh Bellofram).

6.2 Cell lines

MAF cells were cultivated at 37°C, 5% CO_2 in DMEM medium containing 10% fetal calf serum and 4 mM L-glutamine. K562 cells (ATCC: CCL-243) were cultivated at 37°C, 5% CO_2 in RPMI medium containing 10% fetal calf serum and 4 mM L-glutamine. Cells were regularly passaged every three days and kept in the exponential growth phase.

6.3 Transfection

For transfection experiments the coding sequence of human lamin A was fused to a 6x polyhistidine-tag and inserted into the multiple cloning site of the pIRES NEO3 vector system (Clonetech). *Lmna*-deficient mouse adult fibroblasts were transfected utilizing Lipofectamine LTX (Invitrogen) the procedure was performed according to the manufactures manual. For the generation of stable expressing MAF cell lines, cells were selected using 1 mg/ml G418 (Sigma). K562 cells were stably infected utilising a 3rd generation lentivirus system. The expression plasmid pVLX containing the coding sequence of lamin A fused to eGFP was mixed with the helper plasmids psPAX2 and pMD2.G and transfected into 293T cells. Lentivirus containing supernatant was harvested 24h after transfection daily for the next three days and pooled. Supernatant was used 1:1 diluted in RPMI for the infection of K562 cells. Stable expressing cells were selected utilising 2 ug/ml puromycin. To get different expression levels, high and low expressing cells where FACS sorted based on the intensity of the eGFP signal in the green channel.

6.4 Cell preparation and stretching

In general, $5x10^6$ cells were harvested and washed 3 times in PBS (Life Technologies). Cells were loaded into the sample vial of the system and a pressure was applied to the vial to flush the cells into the device. Once cells were flowing past the trapping region, a balancing pressure was applied to the other vial using the electronic regulator. The pressure of the inlet was manually adjusted to control the flow rate of the cells and allow a single cell to be positioned, stationary in the trapping region. Observation of the cells was performed using an inverted microscope (SP5, Leica microsystems) with a 63x/1.2NA objective (Leica microsystems). When the laser power was turned on, the cell is drawn into the centre of the trap where it was held against gravity.

Cells were initially trapped using 500 mW of power from the laser, which results in 190 mW of power in each fibre after splitting the beam in two and the associated losses are taken into account. Once the position and orientation were stable, a stretch sequence was applied, consisting of 4 s of trapping at with a total power in the trap of 380 mW, 4 s of stretching at 2.2 W, and 4 s of relaxation at 380 mW. These values are consistent with previous optical stretching measurements to measure cell and nuclear mechanics[22], and previous studies have shown that the majority of cells remain viable after exposure to such a stretch[30]. Transmission or fluorescence images of the cells were collected using either the LAS (Leica microsystems) package of the microscope running at ~30 frames

per second, or bespoke LabView programs capturing images using a camera (AVT ProSilica) running at ~30 frames per second.

6.5 Nuclear stretching

MAF nuclei were stained using Hoechst® 33342 dye (Fisher Scientific). From Hoechst® dye stock solution (16.23mM) the dye was diluted 1:1000 in media containing the suspended cells ($2x10^6$ cells/ ml). Nuclear stretching was investigated using an inverted EPI-fluorescent microscope (AE31-Motic) with a 40x/0.75NA objective (Olympus) and images were captured by a bespoke LabView program (National Instruments) using a camera (AVT Mako) running at ~30 frames per second.

6.6 Optical stretcher analysis

The boundary of each cell was determined using bespoke edge detection software written in LabView (National Instruments) which detects the edge of the cell and fits an ellipse to it. The change in the ellipse along the stretch axis was measured and formed the deformation curve. Each curve was fitted to a power-law model to describe the viscoelastic behaviour of the cells. Power-law models have been widely used in oscillatory microrheological measurements where the mechanical properties of the cytoskeleton could be modelled as "a glassy material existing close to a glass transition" [48,49]. The response of single cells to external forces has previously been shown to follow a power-law dependence using the uniaxial stretching rheometer [50], micropipette aspiration [38] and in the optical stretcher [51], while nuclear deformations have also been shown to follow power-law responses [37,38,52]. Here, the deformation along the optical axis can be fitted to a two-component power-law model

$$\varepsilon_{(t)} = \varepsilon_0 t^{\beta} + \mathrm{c}$$

where $\varepsilon_{(t)}$ is the time-dependant deformation, ε_0 is the amplitude of the initial deformability, β is a measure of the viscoelasticity of the cell, where a value of 0 represents a purely elastic deformation while a value of 1 represents a purely viscous deformation and c is a fitting constant. Although a power-law model is a good fit for the cellular data presented here for 4s of deformation, care must be taken when extrapolating the behaviour as the time invariance of the power law implies that the deformation will continue indefinitely, which is not representative for biological cells which will generally show a plateau after some time. Such a plateau is clearly visible in the nuclei data, and so a more detailed model was used to fit the nuclei stretch response. The Zener model, consisting of a spring in parallel with a spring and dashpot in series was the simplest model which fitted well and has been demonstrated as a good fit for nuclear deformations[40]. The time-dependent deformation is given by

$$\epsilon_{(t)} = \frac{1}{E_1} + \frac{1}{E_2}\left(1 - e^{-\frac{E_2}{\eta}t}\right)$$

where E_1 and E_2 are related to the instantaneous elastic deformation while η is related to the time-dependant viscous deformation.

6.7 Immunoblot analysis

Whole cell lysates from 10^4 cells were separated utilizing 10 % SDS gels. The protein was transferred to PVDF membranes using a tank blot system with a borate based buffer system. Afterwards the membranes where blocked with 5% milk protein and probed with a lamin A/C antibody[53]. Alpha-tubulin and beta-actin where detected using commercial available antibodies (Sigma-Aldrich, T9026 and A3853 respectively). The detection of all proteins was done on a single membrane at once with an Odyssey FC detection system (LI-COR Biotechnology) utilising enhanced chemiluminescence. Measurement of lamin expression levels were normalised to actin to account for variability in cell loading.

References

[1] K. Mekhail, D. Moazed, *Nat. Rev. Mol. Cell Biol.* **2010**, *11*, 317.
[2] M. Crisp, Q. Liu, K. Roux, J. B. Rattner, C. Shanahan, B. Burke, P. D. Stahl, D. Hodzic, *J. Cell Biol.* **2006**, *172*, 41.
[3] Y. Gruenbaum, R. Foisner, *Annu. Rev. Biochem.* **2015**, *84*, 131.
[4] C. Y. Ho, J. Lammerding, *J. Cell Sci.* **2012**, *125*, 2087.
[5] B. Burke, C. L. Stewart, *Nat Rev Mol Cell Biol* **2013**, *14*, 13.
[6] T. Dechat, S. A. Adam, P. Taimen, T. Shimi, R. D. Goldman, *Cold Spring Harb. Perspect. Biol.* **2010**, *2*, 1.
[7] T. A. Dittmer, T. Misteli, *Genome Biol.* **2011**, *12*, 222.
[8] J. L. V Broers, E. A. G. Peeters, H. J. H. Kuijpers, J. Endert, C. V. C. Bouten, C. W. J. Oomens, F. P. T. Baaijens, F. C. S. Ramaekers, *Hum. Mol. Genet.* **2004**, *13*, 2567.
[9] G. L. Aebi U, Cohn J, Buhle L, *Nat. Lett.* **1986**, 560.
[10] V. L. R. M. Verstraeten, J. L. V Broers, F. C. S. Ramaekers, M. a M. van Steensel, *Curr. Med. Chem.* **2007**, *14*, 1231.

[11] B. van Steensel, J. Kind, *Nucleus* **2014**, *5*, 14.
[12] M. Zwerger, D. E. Jaalouk, M. L. Lombardi, P. Isermann, M. Mauermann, G. Dialynas, H. Herrmann, L. L. Wallrath, J. Lammerding, *Hum. Mol. Genet.* **2013**, *22*, 2335.
[13] A. Jagielska, A. L. Norman, G. Whyte, K. J. Van Vliet, J. Guck, R. J. M. Franklin, K. J. Van Vliet, *Stem Cells Dev.* **2012**, *21*, 2905.
[14] J. Swift, I. L. Ivanovska, a. Buxboim, T. Harada, P. C. D. P. Dingal, J. Pinter, J. D. Pajerowski, K. R. Spinler, J.-W. Shin, M. Tewari, F. Rehfeldt, D. W. Speicher, D. E. Discher, *Science* **2013**, *341*, 1240104.
[15] C. T. Lim, M. Dao, S. Suresh, C. H. Sow, K. T. Chew, *Acta Mater.* **2004**, *52*, 1837.
[16] A. R. Bausch, F. Ziemann, A. A. Boulbitch, K. Jacobson, E. Sackmann, *Biophys. J.* **1998**, *75*, 2038.
[17] O. Otto, P. Rosendahl, A. Mietke, S. Golfier, C. Herold, D. Klaue, S. Girardo, S. Pagliara, A. Ekpenyong, A. Jacobi, M. Wobus, N. Töpfner, U. F. Keyser, J. Mansfeld, E. Fischer-Friedrich, J. Guck, *Nat. Methods* **2015**, *12*, 199.
[18] D. R. Gossett, H. T. K. Tse, S. a Lee, Y. Ying, A. G. Lindgren, O. O. Yang, J. Rao, A. T. Clark, D. Di Carlo, *Proc. Natl. Acad. Sci. U. S. A.* **2012**, *109*, 7630.
[19] H. T. K. Tse, D. R. Gossett, Y. S. Moon, M. Masaeli, M. Sohsman, Y. Ying, K. Mislick, R. P. Adams, J. Rao, D. Di Carlo, *Sci. Transl. Med.* **2013**, *5*, 212ra163.
[20] J. Guck, R. Ananthakrishnan, T. J. Moon, C. C. Cunningham, J. Käs, *Phys. Rev. Lett.* **2000**, *84*, 5451.
[21] A. E. Ekpenyong, G. Whyte, K. Chalut, S. Pagliara, F. Lautenschläger, C. Fiddler, S. Paschke, U. F. Keyser, E. R. Chilvers, J. Guck, *PLoS One* **2012**, *7*, e45237.
[22] K. J. Chalut, M. Höpfler, F. Lautenschläger, L. Boyde, C. J. Chan, A. Ekpenyong, A. Martinez-Arias, J. Guck, *Biophys. J.* **2012**, *103*, 2060.
[23] F. Lautenschläger, S. Paschke, S. Schinkinger, A. Bruel, M. Beil, J. Guck, *Proc. Natl. Acad. Sci. U. S. A.* **2009**, *106*, 15696.
[24] C. J. Chan, A. E. Ekpenyong, S. Golfier, W. Li, K. J. Chalut, O. Otto, J. Elgeti, J. Guck, F. Lautenschläger, *Biophys. J.* **2015**, *108*, 1856.
[25] K. Seltmann, A. W. Fritsch, J. A. Käs, T. M. Magin, *Proc. Natl. Acad. Sci. U. S. A.* **2013**, *110*, 18507.
[26] A. Constable, J. Kim, J. Mervis, F. Zarinetchi, M. Prentiss, *Opt. Lett.* **1993**, *18*, 1867.
[27] J. Guck, R. Ananthakrishnan, H. Mahmood, T. J. Moon, C. C. Cunningham, J. Käs, *Biophys. J.* **2001**, *81*, 767.
[28] B. Lincoln, S. Schinkinger, K. Travis, F. Wottawah, S. Ebert, F. Sauer, J. Guck, *Biomed. Microdevices* **2007**, *9*, 703.
[29] T. Kolb, S. Albert, M. Haug, G. Whyte, *J. Biophotonics* **2014**, *8*.
[30] F. Wetzel, S. Rönicke, K. Müller, M. Gyger, D. Rose, M. Zink, J. Käs, *Eur. Biophys. J.* **2011**, *40*, 1109.
[31] K. C. Neuman, E. H. Chadd, G. F. Liou, K. Bergman, S. M. Block, *Biophys. J.* **1999**, *77*, 2856.
[32] H. Liang, K. T. Vu, P. Krishnan, T. C. Trang, D. Shin, S. Kimel, M. W. Berns, *Biophys. J.* **1996**, *70*, 1529.
[33] T. Sullivan, D. Escalante-Alcalde, H. Bhatt, M. Anver, N. Bhat, K. Nagashima, C. L. Stewart, B. Burke, *J. Cell Biol.* **1999**, *147*, 913.
[34] J. S. H. Lee, C. M. Hale, P. Panorchan, S. B. Khatau, J. P. George, Y. Tseng, C. L. Stewart, D. Hodzic, D. Wirtz, *Biophys. J.* **2007**, *93*, 2542.
[35] J. R. Lange, J. Steinwachs, T. Kolb, L. a Lautscham, I. Harder, G. Whyte, B. Fabry, *Biophys. J.* **2015**, *109*, 26.
[36] J. Lammerding, L. G. Fong, J. Y. Ji, K. Reue, C. L. Stewart, S. G. Young, R. T. Lee, *J. Biol. Chem.* **2006**, *281*, 25768.
[37] J. D. Pajerowski, K. N. Dahl, F. L. Zhong, P. J. Sammak, D. E. Discher, *Proc. Natl. Acad. Sci. U. S. A.* **2007**, *104*, 15619.
[38] F. Guilak, J. R. Tedrow, R. Burgkart, *Biochem. Biophys. Res. Commun.* **2000**, *269*, 781.
[39] A. Vaziri, M. R. K. Mofrad, *J. Biomech.* **2007**, *40*, 2053.
[40] F. Mainardi, G. Spada, *Eur. Phys. J. Spec. Top.* **2011**, *193*, 133.
[41] T. Yang, F. Bragheri, P. Minzioni, *Micromachines* **2016**, *7*, 90.
[42] E. Hatch, M. Hetzer, *J. Cell Biol.* **2014**, *205*, 133.
[43] C. López-Otín, M. A. Blasco, L. Partridge, M. Serrano, G. Kroemer, *Cell* **2013**, *153*, DOI 10.1016/j.cell.2013.05.039.
[44] J.-W. Shin, K. R. Spinler, J. Swift, J. a Chasis, N. Mohandas, D. E. Discher, *Proc. Natl. Acad. Sci. U. S. A.* **2013**, *110*, 188892.
[45] J. Lammerding, P. C. Schulze, T. Takahashi, S. Kozlov, T. Sullivan, R. D. Kamm, C. L. Stewart, R. T. Lee, *J. Clin. Invest.* **2004**, *113*, 370.
[46] K. N. Dahl, S. M. Kahn, K. L. Wilson, D. E. Discher, *J. Cell Sci.* **2004**, *117*, 4779.
[47] A. C. Rowat, D. E. Jaalouk, M. Zwerger, W. L. Ung, I. A. Eydelnant, D. E. Olins, A. L. Olins, H. Herrmann, D. A. Weitz, J. Lammerding, *J. Biol. Chem.* **2013**, *288*, 8610.
[48] B. Fabry, G. N. Maksym, J. P. Butler, M. Glogauer, D. Navajas, J. J. Fredberg, *Phys. Rev. Lett.* **2001**, *87*, 1.
[49] B. Fabry, G. N. Maksym, J. P. Butler, M. Glogauer, D. Navajas, N. A. Taback, E. J. Millet,

J. J. Fredberg, *Phys. Rev. E* **2003**, *68*, 041914.
[50] N. Desprat, A. Richert, J. Simeon, A. Asnacios, *Biophys. J.* **2005**, *88*, 2224.
[51] J. M. Maloney, D. Nikova, F. Lautenschläger, E. Clarke, R. Langer, J. Guck, K. J. Van Vliet, *Biophys. J.* **2010**, *99*, 2479.
[52] K. N. Dahl, A. J. Engler, J. D. Pajerowski, D. E. Discher, *Biophys. J.* **2005**, *89*, 2855.
[53] S. K. Geiger, H. Bär, P. Ehlermann, S. Wälde, D. Rutschow, R. Zeller, B. T. Ivandic, H. Zentgraf, H. A. Katus, H. Herrmann, D. Weichenhan, *J. Mol. Med. (Berl).* **2008**, *86*, 281.